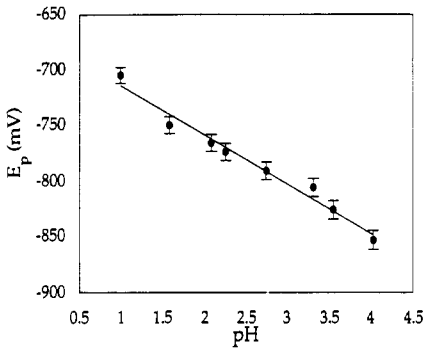

Figure 4. Plot of E_p vs pH for 0.1 M phosphate buffer solutions of **1** (5 mM). A least-squares fit gives the solid line with a slope of 45 mV/pH unit.

As expected from our hypothesis, this is indeed the case. Figure 2 shows the cyclic voltammogram of **1** in DMF in the presence and absence of CF_3CH_2I. Clearly, electrocatalytic reduction of the alkyl iodide occurs upon reaching the $[Ni^{II}L]^{2+}/[Ni^{II}L^{\bullet-}]^{+}$ couple. Again, one-electron reduction of the ligand bound to Ni(II) activates the metal center toward electrophiles. Reaction of an electrophile E^+ with $[Ni^{II}L^{\bullet-}]^+$ would be expected to give $[E\text{-}Ni^{III}L]^+$. Efforts to characterize intermediates in this system are underway, but have not so far been successful. Paramagnetic hydrides and alkyls are rather rare in part because characterization of these unstable species is difficult. In DMF, the $[Ni^{II}L^{\bullet-}]^+$ species initiates electrocatalysis with the more reactive electrophile, CF_3CH_2I, but not with the proton. Electrocatalytic reduction of H^+ is observed in aqueous solution, possibly because acid-base equilibrium is required.

Cyclic Voltammetry in Aqueous Solution. In aqueous solution at a glassy-carbon working electrode, catalytic currents resulting from H_2 evolution are observed for the reduction of **1** (Figure 3). The catalytic currents for both cathodic peaks are linearly dependent on the concentration of **1** with a zero intercept, suggesting a mechanism that is monomolecular in catalyst. Furthermore, the peak current varies linearly with $v^{1/2}$, ruling out electrode adsorption from the electrocatalytic mechanism.[11] Sauvage et al. have shown that electrode adsorption lowers the potential of electrocatalytic H^+ reduction by Ni(II/I) couples in aqueous solution.[8]

The shoulder at ~-0.9 V (Figure 3) can be further resolved using square-wave voltammetry.[12] The E_p for the square-wave voltammogram is pH-dependent, with a slope of 45 mV/pH unit (Figure 4). The value observed here is intermediate between what we would expect for a $1e^-/1H^+$ reduction, such as would be seen if the protonation gave a Ni^{III}-H species, and a $1e^-/2H^+$ reduction, as would be observed if protonation gave the dihydrogen complex, Ni^{III}-H_2.[11] The intermediate value may result from the presence of two pathways or from the failure of square-wave voltammetry to resolve the appropriate potential. Nonetheless, our observations that the catalytic current is first order in **1** and that the peak potential becomes more negative with increasing pH are consistent with either of these pathways, but not one involving a dinuclear Ni complex.

Controlled-Potential Electrolysis. In order to produce macroscopic quantities of H_2, we moved to controlled-potential electrolysis of pH 2 solutions of **1** at a more negative potential. For example, 12 h of electrolysis at -1.1 V electrolysis resulted in the evolution of 14.2 mL of H_2, the identity of which was confirmed by gas chromatography. A control experiment in the absence of catalyst for 12 h produced only 0.3 mL of H_2. From coulometry, we calculate a total turnover number of 12.7 with a current efficiency for H_2 evolution of >95%.[13]

Mechanism and Biological Relevance. Our measurements in DMF suggest the storage of an electron in L, followed by an outer-sphere protonation step to form a 5-coordinate Ni^{III}-H species. A Ni^{III}-H species has been proposed as the active form in the redox cycle of hydrogenase.[14] In aqueous solution, this species reacts further to produce H_2. The mechanism shown in eqs 3-6 is a working hypothesis consistent with our observations.

$$[Ni^{II}L]^{2+} + e^- \rightleftharpoons [Ni^{II}L^{\bullet-}]^+ \quad (3)$$

$$[Ni^{II}L^{\bullet-}]^+ + H^+ \rightleftharpoons [H\text{-}Ni^{III}L]^{2+} \quad (4)$$

$$[H\text{-}Ni^{III}L]^{2+} + e^- + H^+ \rightleftharpoons [H_2\text{-}Ni^{II}L]^{2+} \quad (5)$$

$$[H_2\text{-}Ni^{II}L]^{2+} \rightleftharpoons [Ni^{II}L]^{2+} + H_2 \quad (6)$$

Acknowledgment. We thank the National Institutes of Health for a grant (R.H.C.). H.H.T. thanks the Camille and Henry Dreyfus Foundation for a New Faculty Award, the NSF for a Presidential Young Investigator Award (CHE-9157411), the David and Lucile Packard Foundation for a Fellowship in Science and Engineering, and the donors of the Petroleum Research Fund, administered by the American Chemical Society, for partial support of this research.

(12) O'Dea, J.; Osteryoung, J.; Osteryoung, R. A. *Anal. Chem.* **1981**, *53*, 1981.

(13) After the electrolysis, there is no evidence of any hydrogenated ligand product by optical spectroscopy, again supporting the involvement of Ni in the catalytic reaction.

(14) Fan, C.; Teixeira, M.; Moura, J. J. G.; Moura, I.; Huynh, B. H.; LeGall, J.; Peck, J. D., Jr.; Hoffman, B. M. *J. Am. Chem. Soc.* **1991**, *113*, 20.

Contribution from the Department of Chemistry, University of Illinois at Chicago, Chicago, Illinois 60680, and ICMA, CSIC—University of Zaragoza, Zaragoza, Spain

Magnetochemistry of the Tetrahaloferrate(III) Ions. 3. Specific Heat of Bis[4-bromopyridinium tetrachloroferrate(III)]-4-Bromopyridinium Chloride

Roey Shaviv,[1a] K. E. Merabet,[1a] D. P. Shum,[1a] C. B. Lowe,[1a] D. Gonzalez,[1b] R. Burriel,[1b] and Richard L. Carlin*[,1a]

Received July 30, 1991

Introduction

The crystal structure and magnetic susceptibilities of bis[4-bromopyridinium tetrachloroferrate(III)]-4-bromopyridinium chloride were recently reported.[2] This substance is a canted antiferromagnet, ordering at 2.34 K, and is one of a large series of related materials.[2-5]

The specific heat of a system is an important indicator of cooperative magnetic behavior.[6] Thus, the observation of a λ-anomaly indicates that a phase transition has taken place and identifies precisely the transition temperature, while broad maxima are generally indicative of the presence of substantial short-range order.

Though the existence of pairs of metal ions was apparent in the crystal structure of 2[4-Br(py)H][$FeCl_4$]·[4-Br(py)H]Cl, there was no noticeable contribution of short-range order to the susceptibility of the compound. We present here strong evidence,

(1) (a) University of Illinois at Chicago. (b) CSIC—University of Zaragoza.

(2) Zora, J. A.; Seddon, K. R.; Hitchcock, P. B.; Lowe, C. B.; Shum, D. P.; Carlin, R. L. *Inorg. Chem.* **1990**, *29*, 3302.

(3) Lowe, C. B.; Carlin, R. L.; Schultz, A. J.; Loong, C.-K. *Inorg. Chem.* **1990**, *29*, 3308.

(4) Lowe, C. B. Dissertation, University of Illinois at Chicago, 1990.

(5) Carlin, R. L.; Lowe, C. B.; Palacio, F. P. *An. Quim.* **1991**, *87*, 5.

(6) Carlin, R. L. *Magnetochemistry*; Springer-Verlag: Berlin, 1986.

0020-1669/92/1331-1724$03.00/0

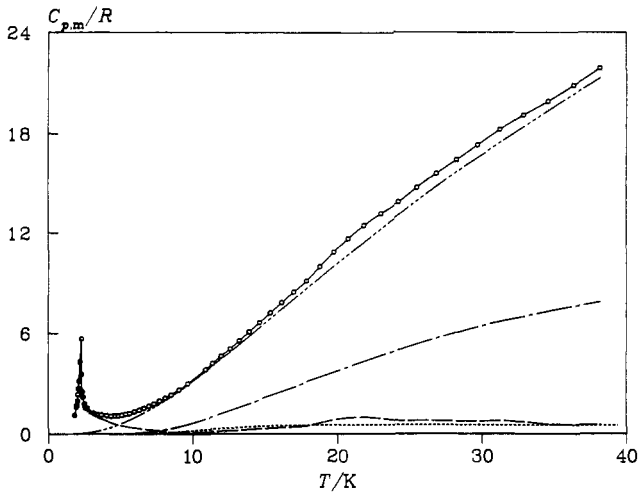

Figure 1. Molar specific heat of $[4\text{-Br(py)H}]_3Fe_2Cl_9$: (o–o) experimental results; (——) lattice specific heat; (–·–) specific heat of internal modes as represented by two Einstein functions (this specific heat is a part of the lattice contribution); (– – –) specific heat of magnetic dimers; (– –) excess specific heat (see text).

obtained from specific heat measurements and their analysis, in favor of such an interaction.

Experimental Section

The synthesis of the sample was described, along with chemical analysis data, in the preceding paper in this series.[2] The same single-crystal samples used for the previous study were used here, but they were crushed and pelleted to fit inside the calorimeter. To facilitate rapid thermal equilibrium, prior to pelleting, the sample was threaded with about 0.2 g of copper wires, whose thermal diffusivity is much larger than that of the sample. Thermal contact between the sample and the calorimeter was achieved by applying a thin layer of Apiezon N grease on the calorimeter interior. The specific heat of the excess Apiezon N grease[7] and copper[8] were subtracted from the total specific heat for the analysis of the data.

Full details concerning the construction of a new adiabatic calorimeter are provided in the supplementary material.

Results and Discussion

The experimental specific heat of $[4\text{-Br(py)H}]_3Fe_2Cl_9$ is plotted in Figure 1 and tabulated in Table S1. A λ-type phase transition associated with the onset of long-range ordering is observed. The maximum specific heat associated with the transition was found at 2.280 ± 0.005 K, which is identified as the critical temperature.

The lattice contribution to the specific heat of $[4\text{-Br(py)H}]_3Fe_2Cl_9$ was determined by means of the Komada–Westrum (KW) phonon distribution model.[9-12] The application of the model to several chemical systems has been demonstrated before with remarkable results.[13-18] A review of the model is beyond the scope of this article, and the reader is referred to refs 9–18 for a more detailed discussion concerning the model and its application. A brief description, however, is in order. The model calculates an approximate phonon density of states which is obtained on the basis of physical properties such as atomic masses, structural information, and the specific heat. In addition to acoustic branches (which are represented in the Debye model, although the present model treats them somewhat differently) and internal branches (the Einstein model), this model also allows for the incorporation of optical branches and thus provides a more physically realistic approximation to the "real" density of states function. We have enhanced the application of the model by the incorporation of graphics and by simplifying the input/output procedures. The new program, adapted for DOS, was used for the calculations presented here.

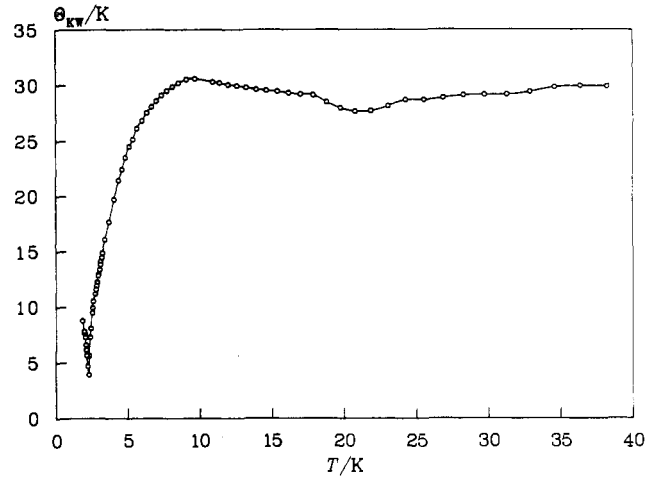

Figure 2. Apparent characteristic temperature Θ_{KW} for $[4\text{-Br(py)H}]_3Fe_2Cl_9$.

The phonon density of states function which results from the calculation is represented by the apparent characteristic temperature, Θ_{KW}. A constant apparent Θ_{KW} as a function of temperature indicates that the calculation results in the same phonon distribution function over an extended temperature region. One may, therefore, conclude that the experimental specific heat consists only of a lattice contribution over that temperature region. A minimum for Θ_{KW} will be observed if excess contributions are present. The quantity Θ_{KW} may be interpolated over, or extrapolated to, regions in which excess contributions are present, and as a result an excellent approximation to the lattice contribution may be obtained.

The apparent characteristic temperature Θ_{KW} for $[4\text{-Br(py)H}]_3Fe_2Cl_9$ is presented in Figure 2. A sharp decrease in Θ_{KW} is detected below 9 K, as expected in the transition region. A second, broader minimum in Θ_{KW} is observed in the vicinity of 21 K, indicating additional excess specific heat contributions around that temperature. This excess specific heat contribution is believed to be that of magnetic dimers, which results in a Schottky-like specific heat contribution. The theoretical specific heat of magnetic dimers was given by Smart[19] and by Ginsberg.[20] For such an interaction the magnetic exchange constant J'/k_B turns out to be uniquely determined by the maximum in the excess specific heat and on the total spin S ($|J'|k_B = 1.24T_{max}$ for $S = {}^5/_2$).[20] For Fe(III), $S = {}^5/_2$ and therefore $J'/k_B = -26.7$ K. The specific heat associated with the pair-wise interaction appears as the dashed line in Figure 1. The physical origin of these dimer interactions is the paired arrangement of the $[FeCl_4]^-$ tetrahedra in the unit cell. Two distinct iron atoms exist in the material. The nearest iron–iron distance was reported as 6.567 Å for $[4\text{-Cl(py)H}]Fe_2Cl_9$, which is 1.069 Å shorter than the second nearest iron distance. The substance $[4\text{-Br(py)H}]_3Fe_2Cl_9$ is isostructural with $[4\text{-Cl(py)H}]_3Fe_2Cl_9$, and iron-iron interactions are expected to be similar for both compounds. Short-range magnetic ordering associated with magnetic dimers is not observed for $[4\text{-Cl(py)H}]_3Fe_2Cl_9$, however.

(7) Wun, M; Phillips, N. E. *Cryogenics* **1975**, 36. Berolo, J. *Cryogenics* **1974**, 601.
(8) White, G. K.; Collocot, S. J. *J. Phys. Chem. Ref. Data* **1984**, *13*, 1251.
(9) Komada, N. Dissertation, University of Michigan 1985.
(10) Komada, N. *Netsu Sokuti* **1990**, *17*, 25.
(11) Komada, N.; Westrum, E. F., Jr. To be published.
(12) Komada, N.; Westrum, E. F., Jr. *Thermochim. Acta* **1988**, *109*, 11.
(13) Shaviv, R. Dissertation, University of Michigan, 1988.
(14) Shaviv, R.; Westrum, E. F., Jr.; Fjelvag, H.; Kjekshus, A. *J. Solid State Chem.* **1989**, *81*, 103.
(15) Shaviv, R.; Westrum, E. F., Jr.; Brown, R. J. C.; Sayer, M.; Yu, X.; Weir, R. D. *J. Chem. Phys.* **1990**, *92*, 6794.
(16) Shaviv, R.; Westrum, E. F., Jr.; Gronvold, F.; Stolen, S.; Chihara, H.; Inaba, A. *J. Chem. Thermodyn.* **1989**, *21*, 63.
(17) Konings, R. J. M.; Cordfunke, E. H. P.; Westrum, Jr., E. F.; Shaviv, R. *J. Phys. Chem. Solids* **1990**, *51*, 439.
(18) Shaviv, R.; Westrum, E. F., Jr.; Gruber, J. B.; Beaudry, B. J. *J. Chem. Phys.*, in press.
(19) Smart, J. S. In *Magnetism*; Rado, G. T., Suhl, H., Eds.; Academic Press: New York, 1963; Vol. III, p 63.
(20) Ginsberg, A. P. *Inorg. Chim. Acta Rev.* **1971**, *5*, 45.

A second source of abnormally high specific heat at low temperatures is the low frequency vibrations of the 4-bromopyridinium groups. These vibrations are thermally activated at relatively low temperatures, and their specific heat may be best described by Einstein functions. Thus two weighted Einstein frequencies were incorporated into the Komada-Westrum approximation for the lattice specific heat as internal branches at 38 and 72 cm^{-1}. We note that we have no spectroscopic evidence for these values, and their selection was arbitrary and served to achieve a fit between the sum of all contributions and the experimental results. However, thermal activation of low-frequency vibrations at low temperatures, although not very common, is known and has been reported for ammonium salts[21-23] and several silver compounds.[16] The apparent characteristic temperature Θ_{KW}, presented in Figure 2, was calculated by taking these internal modes into account. A constant Θ_{KW} equal to 31.1 K was established as the characteristic temperature for $[4\text{-Br(py)H}]_3Fe_2Cl_9$ and was used to calculate the lattice specific heat between 0 and 38 K. The resulting lattice contribution to the specific heat is also presented in Figure 1.

Once the lattice specific heat is calculated, the excess specific heat is readily obtained. This excess specific heat is also shown in Figure 1 and is believed to originate solely from magnetic ordering phenomena. The broad maximum at higher temperatures appears to agree well with the theoretical prediction for magnetic dimers and therefore may be interpreted as such. The λ-type transition at lower temperatures is associated with canted antiferromagnetic ordering of the Fe(III) ions.[2] The magnetic entropy between 0 and 9.0 K, $\Delta_m S^0$, is found to be $(1.887 \pm 0.05)R$. The theoretical value for the entropy of disorder corresponding to two $S = {}^5/_2$ ions is $2R \ln (2S + 1) = 2R \ln 6 = 3.58R$. This value is about twice as large as the experimental entropy of transition. The rest of the entropy has to be included in the Schottky-like anomaly due to the stronger pair exchange constant. Less than half of the disorder process takes place below the peak temperature, 2.280 K. The tail of the transition extends up to 9.0 K with a corresponding post-transition entropy of $1.036R$. This indicates that short-range interactions play an important role in the magnetic ordering process.

The transition temperature, 2.280 K, is lower than that previously reported, 2.34 K.[2] The origin of the shift in T_c may be attributed to mechanical stress afflicted on the samples prior to the calorimetric measurement.

The tail of the transition (i.e., the magnetic specific heat at temperatures higher than T_c) follows a T^{-2} behavior as expected.[24] However, the presence of a large degree of short-range order precludes the use of the T^{-2} dependence of the magnetic specific heat, according to Domb and Miedema,[24] for the evaluation of the exchange constant. Previously,[2] the compound has been interpreted as an Heisenberg antiferromagnet based upon its magnetic susceptibility and the exchange constant J/k_B was determined to be between -0.111 and -0.094 K. From the critical point determined here, 2.280 K, we find that $J/k_B = -0.114$ K, in good agreement with the previous report.

Acknowledgment. This research was supported by the Solid State Chemistry program of the Division of Materials Research of the National Science Foundation, through Grant DMR-8815798, as well as by the CICYT, Grant MAT 89-531. We wish to extend our gratitude to Mr. John Costa for invaluable assistance in the cryostat assembly.

Supplementary Material Available: Text giving a complete description of the calorimeter, a figure depicting the calorimeter, and a table of specific heats as a function of temperature (9 pages). Ordering information is given on any current masthead page.

(21) Brown, R. J. C.; Callanan, J. E.; Weir, R. D.; Westrum, E. F., Jr. *J. Chem. Phys.* **1986**, *85*, 5963.
(22) Brown, R. J. C.; Weir, R. D.; Westrum, E. F., Jr. *J. Chem. Phys.* **1989**, *91*, 391.
(23) Brown, R. J. C.; Callanan, J. E.; Weir, R. D.; Westrum, E. F., Jr. *J. Chem. Thermodyn.* **1987**, *19*, 1173.
(24) Domb, C.; Miedema, A. R. *Prog. Low Temp. Phys.* **1964**, *4*, 269.

Contribution from the Departament de Química Inorgànica, Universitat de Barcelona, Diagonal 647, 08028-Barcelona, Spain, and Departament de Cristal.lografia i Mineralogia, Universitat de Barcelona, Martí Franquès s/n, 08028-Barcelona, Spain

The First Nickel(II) Alternating Chain with Two Different End-to-End Azido Bridges

Ramon Vicente,*[†] Albert Escuer,[†] Joan Ribas,[†] and Xavier Solans[‡]

Received July 30, 1991

Introduction

In a uniform linear-chain system, the intrachain exchange constant has been assumed not to vary with position. That is, the Hamiltonian used is

$$H = -J(S_{i-1}S_i + \alpha S_i S_{i+1})$$

with $\alpha = 1$. An alternating chain is defined for $\alpha < 1$. When $\alpha = 0$, the model is reduced to the dimer model with pairwise interaction. The preparation and properties of $S = {}^1/_2$ alternating chains has been of continuous interest for some years,[1] and there is a large body of results. Some examples of the previously reported complexes are $[Cu(\gamma\text{-picoline})_2Cl_2]$,[2] $[Cu(N\text{-methylimidazole})_2Br_2]$,[3] $Cu(NO_3)_2 \cdot 2.5H_2O$,[4] and [Cu(hfa)$_2$TEMPOL].[5] With $S > {}^1/_2$, alternating chains are very scarce. Some of these chains are only found with alternating g factors, but not with $\alpha < 1$.[6] To our knowledge, only one case has been fully characterized: *catena*-(μ-oxo)hemi(porphyrazinato)iron(IV).[7] Consequently, no Ni(II) alternating chain has been reported. In order to study alternating chains of Ni(II), one of the ligands which may give good results is the N_3^- anion, because it is well established that it can bridge metal ions in two modes (double-bridging end-on or end-to-end)[8] and when the blocking ligands for Ni(II) are tridentate, the sixth position of each nickel atom is occupied by a terminal azido group.[9] These can consequently be potentially considered as blocks which can be linked together in a 1D alternating system. By using this strategy, we report here the synthesis and crystal structure of the first Ni(II) alternating chain with the N_3^- entity acting as an end-to-end bridge in two different modes, double and simple bridges, respectively: *catena*-$[Ni_2(\mu\text{-}N_3)_3(dpt)_2](ClO_4)$, where dpt is the tridentate amine ligand bis(3-aminopropyl)amine. We have also measured the magnetic susceptibility of this compound between room temperature and 4 K. The magnetic behavior confirms that this chain is the first magnetically alternating Ni(II) chain.

Experimental Section

Materials. Bis(3-aminopropyl)amine (Fluka) and nickel perchlorate (Fluka) were purchased and used without purification. The dinuclear μ-azido-bridged compound $[Ni_2(\mu\text{-}N_3)_2(Me_3[12]N_3)_2](ClO_4)_2$ (Me_3-[12]N_3 = 2,4,4-*trimethyl*-1,5,9-*triazacyclododec*-1-ene) was previously prepared.[10]

Synthesis. *Caution!* Perchlorate salts of metal complexes with organic ligands are potentially explosive. Only a small amount of materials should be prepared, and they should be handled with caution.

If an aqueous solution of nickel perchlorate hexahydrate, bis(3-aminopropyl)amine (dpt), and sodium azide in the molar ratio 1:1:3 is left at room temperature for several days, water-soluble blue crystals of *catena*-$[Ni_2(\mu\text{-}N_3)_3(dpt)_2](ClO_4)$ are obtained. On the other hand, when 0.5 g of the dinuclear azido-bridged compound $[Ni_2(\mu\text{-}N_3)_2(Me_3[12]N_3)_2](ClO_4)_2$[10] is dissolved in 100 mL of a 0.1 M solution of aqueous sodium azide, blue single crystals of the same compound *catena*-$[Ni_2(\mu\text{-}N_3)_3(dpt)_2](ClO_4)$ are also obtained after very slow evaporation of the solvent. The two products were characterized to be the same using spectral measurements and elemental analysis. The second synthetic pathway implies the cleavage of the bonded macrocycle in basic medium, yielding acetone and dpt. This cleavage has been previously reported by Curtis et al.[11] for similar macrocyclic compounds.

[†] Departament de Química Inorgànica.
[‡] Departament de Cristal.lografia i Mineralogia.

0020-1669/92/1331-1726$03.00/0